

Exact treatment of Ising model on the helical tori

Tsong-Ming Liaw

Computing Centre, Academia Sinica, 11529 Taipei, Taiwan

Ming-Chang Huang^y and Yen-Liang Chou

Department of physics, Chung-Yuan Christian University, Chungli, Taiwan

Simon C. Lin

Institute of Physics, Academia Sinica, 11529 Taipei, Taiwan

Feng-Yin Li

Department of Chemistry, National Chung-Hsing University, Taichung, Taiwan

(Dated: March 23, 2024)

The exact closed forms of the partition functions of 2D Ising model on square lattices with twisted boundary conditions are given. The constructions of helical tori are unambiguously related to the twisted boundary conditions by virtue of the $SL(2; \mathbb{Z})$ transformations. Numerical analyses reveal that the finite size effect is irrelevant to the chirality equipped with each helical boundary condition.

PACS numbers:

Since Onsager obtained the exact solution of the two-dimensional (2D) Ising model with cylindrical boundary condition (BC) in 1944 [1], the exact treatments of Ising models on different 2D surfaces have been continuously attempted. Most recently, Wu and Lu [2] have provided analytical treatments for the Ising models with BCs of particular class, including Möbius strip, Klein bottle and self-dual BC. The exact study of the model subject to BCs is of fundamental importance. First, it represents new challenges for the unsolved lattice-statistical problems [1, 2, 3, 4, 5, 6, 7, 8, 9, 10]. Second, it is crucial for the finite-size analysis [11, 12, 13, 14, 15]. Furthermore, it provides an optimal testbed for the predictions of the conformal field theory [16]. Numerical simulations are plausible for the exact analyses and provide very rich content for the theory of finite-size scalings [12]. For example, based on the exact analysis of dimer statistics, by Wu and Lu ([2], 1998), Kaneda and Okabe [13] have achieved, via computer simulations, more thorough understanding for the finite-size scaling behaviour of the Ising models subject to the boundary types of Möbius strip and Klein bottle. While interesting numerical studies, concerning the excess number of percolation [14] and the Binder parameter [15], for the Ising model for the twisted BCs further proceed, the problem for lacking the corresponding closed form of the partition functions turns out to be significant.

Boundary conditions are prescribed by sets of primitive vectors which impose the periodicity on the corresponding directions. For definite BC, sets of primitive vectors are by no means unique [18]. For 2D, the equivalent transformations among the primitive vector-pairs on lattice essentially preserve the area spanned by the vector-pairs and are thus recognised as $SL(2; \mathbb{Z})$. This is the prototype of the modular symmetry discussed in the context of conformal field theory [16]. The helical BC is of particular significance owing to its geometrical feature and its relevance to the formulation for the nanotube physics [17]. Helical tori are formed by pairwise joining the edges of the sheet spanned by any two orthogonal primitive vectors. The construction ends up with distinct orientations of the underlying lattice, labelled by the chirality [17] as well as the chiral aspect ratio. The conventional periodic BC is referred as the helical BC with trivial chirality, as depicted in Fig. 1. The twisted BC, on the other hand, counts on the modification to the conventional BC by cutting the torus and then rejoining after twisting. Furthermore, the helical BC is shown to be the subclass of twisted one according to the equivalence relations, as depicted in Fig. 2.

In this Letter, the 2D Ising model subject to the twisted BCs is exactly analysed. The general form of such partition functions is obtained, firstly. Symmetry conditions are employed to reduce the redundancy on setting the twisting factor in relation to the conventional aspect ratio A . In addition, any helical BC is shown unambiguously equivalent to a definite twisted BC, by virtue of the $SL(2; \mathbb{Z})$ transform. The finite-size shift of critical temperature is thus investigated numerically. It turns out that the scaling behaviour is found chirality-independent. Meanwhile, in examining the twisting pair dependence, the $A = 1$ scaling rule appears to be twisting-independent. We then conclude by few remarks on the comparison to the previous numerical issues.

Consider a $M \times N$ square lattice with the coordinates of the lattice sites specified in form of $\hat{x}m + \hat{y}n$. The partition

^Electronic address: ltm-ing@gate.sinica.edu.tw

^yElectronic address: m-ing@phys.cycu.edu.tw

function of the Ising model lattice is given as $Z_{M,N} = [2 \cosh(J_1) \cosh(J_2)]^{MN} Q_{M,N}$ with the reduced partition function $Q_{M,N} = \prod_{m=1}^M \prod_{n=1}^N \hat{Q}_{m,n}$, where $\hat{Q}_{m,n} = \frac{1}{2} \sum_{f_{m,n} \in \{0,1\}} [(1 + t_1 a_{m,n} a_{m+1,n}) (1 + t_2 a_{m,n} a_{m,n+1})]$. Here we use the notations, $t_i = \tanh(J_i)$ with J_i , for $i = 1, 2$, denoting the coupling constants along x and y directions, and $\beta = 1/k_B T$. Twisted BCs amount to the identifications of the spin variables whose locations are related by the pair of primitive vectors, say, \vec{a}_1 and \vec{a}_2 . Basically, only two types of twisting should be in considerations: One is referred as $Tw_I(M, N; d=M)$ specified by the primitive vectors $f \vec{a}_1 = M \hat{x} + d \hat{y}$; $\vec{a}_2 = N \hat{y}$, and the other is as $Tw_{II}(M, N; d=N)$ specified by $f \vec{a}_1 = M \hat{x}$; $\vec{a}_2 = d \hat{x} + N \hat{y}$.

According to Pechko [8], (1985), the reduced partition function takes the form of

$$Q_{M,N} = \sum_{f_{m,n} \in \{0,1\}} \prod_{m=1}^M \prod_{n=1}^N e^{a_{m,n} b_{m,n}} [A_{m,n} A_{m+1,n}] \quad (1)$$

with

$$\begin{aligned} A_{m,n} &= \sum_{a_{m,n} \in \{0,1\}} da_{m,n} da_{m,n+1} e^{a_{m,n} a_{m,n+1}} [A_{m,n} A_{m+1,n}] \\ B_{m,n} &= \sum_{b_{m,n} \in \{0,1\}} db_{m,n} db_{m,n+1} e^{b_{m,n} b_{m,n+1}} [B_{m,n} B_{m+1,n}] \end{aligned} \quad (2)$$

where $A_{m,n} = 1 + a_{m,n} a_{m,n+1}$, $A_{m,n+1} = 1 + t_1 a_{m,n} a_{m,n+1}$, $B_{m,n} = 1 + b_{m,n} b_{m,n+1}$ and $B_{m,n+1} = 1 + t_2 b_{m,n} b_{m,n+1}$. In above, two pairs of conjugate Grassmann variables, $f a_{m,n}; a_{m,n}$ and $f b_{m,n}; b_{m,n}$ have been introduced. As technically known to the Refs. [8, 9, 10], the handling of the boundary Boltzmann weights,

$$= \prod_{n=1}^N \prod_{m=1}^M e^{a_{m,n} b_{m,n}} [A_{m,n} A_{m+1,n}] \quad (3)$$

remains central in the treatments. It turns out to be instructive to reexamine the paradigm which solves this problem in the original periodic settings $a_{m+M,n} = a_{m,n}$ and $a_{m,n+N} = a_{m,n}$.

In Ref. [8] (1985), the boundary Boltzmann weights are rearranged such that $j_1 + j_2 + j_3 + j_4$ subject to the BCs, imposed on the Grassmann variables, with

$$= \prod_{n=1}^N \prod_{m=1}^M e^{a_{m,n} b_{m,n}} [A_{m,n} A_{m+1,n}] \quad (4)$$

where the arrows indicate the ordering for the multiplications and we employ the notation \int for all the coming weighted integration over relevant Grassmann variables. Subsequently, minor ordering is applied routinely and furnishes the simple expression of pure Grassmannian integrations,

$$Q_{M,N} = \frac{1}{2} [G j_1 + G j_2 + G j_3 + G j_4]; \quad (5)$$

$$G = \sum_{m,n} \exp \left[a_{m,n} b_{m,n} + t_1 t_2 a_{m,n} b_{m,n+1} + (t_1 a_{m,n} + t_2 b_{m,n+1}) (a_{m,n+1} + b_{m,n}) \right] g; \quad (6)$$

where the integrations can be diagonalised and carried out, straightforward [8].

The reviewing paragraph above suggests that the modification is only essential for the twisted BC in the the key steps, i.e., from Eq. (3) to Eq. (4). For Tw_I , the $\prod_{m=1}^M$ term in Eq. (3) is calibrated in relation to the toroidal one. This then leads to

$$= \prod_{m=1}^M \prod_{k=1}^{N/d} e^{a_{m,k} b_{m,k}} [A_{m,k} A_{m+1,k}] \prod_{k=n/d+1}^N e^{a_{m,k} b_{m,k}} [A_{m,k} A_{m+1,k}] \prod_{n=1}^N \prod_{m=1}^M e^{a_{m,n} b_{m,n}} [A_{m,n} A_{m+1,n}] \quad (7)$$

where the BC $a_{m+M,n+d} = a_{m,n}$ has been explicitly employed. Reordering of the first three products in Eq. (7) is essential such that the form of Eq. (4) can be achieved. By recursive use of the identity for the permutation of Grassmannian functions [8], we employ, instead,

$$XYZ = \frac{1}{2} (ZYX + ZYX + ZYX + ZYX); \quad (8)$$

where $X;Y$ and Z stand for the corresponding three objects and the superscript " " denotes flipping the sign of the Grassmann variables. Accordingly, the form of Eq. (4) is achieved which implies Eq. (5). Note that the form of Eq. (6) preserves under twisting. However, the BCs imposed on the Grassmann variables are modified in response to the corresponding sign flipping appearing in the deduction of Eq.(8). For convenience, the compact notation as $\mathbf{a}_i = (;)$ can be employed as follows. The first sign in the parenthesis corresponds to $a_{m;n} = a_{m;0}$ and the second one is for $a_{m;n+d} = a_{0;n}$. The BCs are given as $\mathbf{a}_1 = (;)$, $\mathbf{a}_2 = (+;)$, $\mathbf{a}_3 = (;+)$ and $\mathbf{a}_4 = (+;+)$. The exact partition function is straightforward, henceforth.

For Tw_I , with $d=M$, the reduced partition function is

$$Q_{M,N} = \frac{1}{2} I_{M,N} \left(\frac{1}{2}; \frac{1}{2} \right) + I_{M,N} \left(\frac{1}{2}; 0 \right) + I_{M,N} \left(0; \frac{1}{2} \right) \text{sgn} \left(\frac{T}{T_c} \right) I_{M,N} (0;0) ; \quad (9)$$

$$I_{M,N} (;) = \prod_{p=1}^M \prod_{q=1}^N \left(\cos 2 \frac{p+}{M} \cos 2 \frac{q+}{N} \right)^{1=2} ; \quad (10)$$

where $\mathbf{a}_0 = (1+t_1^2)(1+t_2^2)$, $\mathbf{a}_1 = 2t_1(1-t_2^2)$ and $\mathbf{a}_2 = 2t_2(1-t_1^2)$. In addition, the function $\text{sgn}(x)$ denotes the sign of the value x and T_c is the critical temperature of the bulk system. The reduced partition function for Tw_{II} remains formally as Eq. (9) but with

$$I_{M,N} (;) = \prod_{p=1}^M \prod_{q=1}^N \left(\cos 2 \frac{p+}{M} \cos 2 \frac{q+}{N} \frac{(p+)}{M} \right)^{1=2} ; \quad (11)$$

where, instead, $d=N$.

It can be checked for Eq. (9) that $Q_{M,N} = Q_{M,N}$ based on either Eq. (10) or Eq. (11), while, intuitively, twisting either clockwise or counterclockwise is not classified by the system. Noteworthy is also that reversing the sign of a twist factor can not be obtained via the $SL(2;Z)$ transform. On employing this transform explicitly, pairs of primitive vectors are related among each other in the manner of

$$\begin{pmatrix} \mathbf{a}_1 \\ \mathbf{a}_2 \end{pmatrix} = M \begin{pmatrix} \mathbf{a}_1 \\ \mathbf{a}_2 \end{pmatrix} \quad SL(2;Z); \quad (12)$$

Consider Tw_I , for example. The choice of matrix elements $M_{11} = 1, M_{12} = J/2Z, M_{21} = 0$ and $M_{22} = 1$ gives rise to the new pairs of primitive vectors $\mathbf{a}_1 = M\hat{x} + (d+N)\hat{y}$; $\mathbf{a}_2 = N\hat{y}$, which prescribes the same BC. As evidence, $Q_{M,N} = Q_{M,N}^{JA}$ can be explicitly checked, where the conventional aspect ratio appears as $A = N/M$. Therefore, the effective range of A is $0 < A$. In addition, the equivalence $\text{Tw}_I(M;N; A=J) = \text{Tw}_{II}(M^0 = JM; N^0 = N=J; \mathbf{a}^0 = 1=)$ can be achieved by virtue of choosing the elements $M_{11} = J/2Z, M_{12} = 1, M_{21} = 1$ and $M_{22} = 0$ with $\mathbf{a}^0 = A=J$ and $\mathbf{a}^0 = J=A$. Again, the partition functions based on Eqs. (10 and (11) appear to fulfill these relations. Hence, it is sufficient to study the unique correspondence of a helical torus to the one of the above twistings, say Tw_I .

The helical tori, on the hand, lie in the orthogonal primitive vector pair,

$$\begin{pmatrix} \mathbf{a}_1 \\ \mathbf{a}_2 \end{pmatrix} = \begin{pmatrix} \hat{x} P_1 + \hat{y} Q_1 \\ \hat{x} Q_2 + \hat{y} P_2 \end{pmatrix}; \quad (13)$$

where the two radii for the torus are given as $L_i = \frac{P_i}{P_1^2 + Q_1^2}$ for $i=1,2$. Hence, let the helical system denoted by $Hl(B;L_1;)$, where the chiral aspect ratio $B = L_2/L_1$ and the chirality $= Q_1/P_1 - Q_2/P_2$. In order to furnish the equivalent structure $Hl(B;L_1;) = \text{Tw}_I(A;M;)$, $M_{11} = P_1/M$ and $M_{21} = Q_2/M$ implies that

$$M_{21} = B M_{11} \quad (14)$$

$$1 = M_{11}M_{22} - M_{21}M_{12}; \quad (15)$$

$$A = \frac{(M_{21})^2}{B} + B (M_{11})^2; \quad (16)$$

$$= \frac{M_{21}M_{22}}{B} - B M_{11}M_{12}; \quad (17)$$

However, few remarks on the uniqueness of the relations above remain essential.

The $[M_{12}; M_{22}]$ pair is unambiguously determined up to M_{11} and M_{21} for $0 < A$. This is because shifting $[M_{12}; M_{22}]$ by appending $[JM_{11}; JM_{21}]$ leaves Eq.(15) invariant $8J/2Z$ but only causes deviation by JA in Eq. (17). Meanwhile, the allowable region for $[M_{12}, M_{22}]$ appropriate for $0 < A$ is exactly one vector section between $M_{11}; M_{21}$. In addition, the ambiguity relating to size dependence can be removed by noting the coprime properties between M_{11} and M_{21} which ensures the solubility of the integer pair $[M_{12}; M_{22}]$ subject to Eq. (15). Consequently, a helical two-tuple $(B;)$ is equipped a unique pair $fA; g$ for the twisting in the effective range. Moreover, the classification of helical via the twisting parameters remains unambiguous. This is because if different helical tori were equivalent to the same twisted BC, $SL(2, Z)$ transformations would have been held among them, which can be shown impossible. The effective range of the helical BC can also be further reduced. The partition function is unable to classify the rolling up direction in forming the tori, hence, no distinction between the characterisations and is essential. Subsequently, once $H(l(B;)) = Tw_I(A;)$, one can derive that $H(l(B; 1) = Tw_I(A;)$. To be concrete, assuming $g > 0$, $g = 1$ implies $M_{11}^0 = M_{21}^0; M_{21}^0 = M_{11}^0$ as well as $M_{12}^0 = M_{22}^0$ and $M_{22}^0 = M_{12}^0$ according to Eq. (14). This then preserves A but gives $g = 1$ by virtue of Eqs. (15) and (16).

The shift of the specific-heat peak T_{max} away from the critical temperature T_c under the isotropic couplings can be computed from the exact partition function. Upon using the parametrisation in terms of $Tw_I(A; M;)$, the critical shift $(A;) = (T_{max}() - T_c) = T_c$ is plotted against $l = L = 1 = \frac{M}{N}$ in Fig. 3. For helical BCs, Eqs. (14)–(17) are employed in order to determine the critical shifts $(B;)$ versus $l = L = 1 = \frac{M}{N}$ for various B s and s , as shown in Fig. 4. In Fig. 3, the curves of scaling for definite A deviate by altering the twist factor s . However, no such splitting is found for the exceptional case $A = 1$. On the other hand, all the critical shifts $(B;)$ with the same B value, in Fig. 4, fall into to one single smooth curve, the finite-size effect turns out to be chirality-independent. Hence, the matching of the two particular curves, i.e. for $B = 1$ in Fig. 3 and for $A = 1$ in Fig. 4, appears to be an additional feature. Moreover, the critical shift $(B;)$ flips its sign at $B = b_0$ and $l = b_0$ with $b_0 \approx 3$, as it was anticipated by Ferdinand and Fisher [1] for the conventional periodic BC, where the exact b_0 value was determined as $b_0 = 3.13927$; a result which now applies for all the helical tori.

In conclusion, we provide the complete description for the finite-size effect of Ising Model subject to the subclass helical BCs of the twisted tori. This is explicitly done by solving the exact form of the partition function appropriate for all the twisted BCs. The evidence of the finite-size effect being chirality-independent basically supports the invariance of the scaling behaviour of partition function under rotation of the primitive vector pair subject to BCs, conjectured in Ref. [15]. However, the particular coincidence for $A = 1$ and $B = 1$ regardless s suggests further interesting points exceeding beyond the rotational invariance. For consistency, we stress the fact that $A = 1$ does not non-trivially permit any helical structure, as one may observe in Eqs. (14)–(17). As the final remark, the invariant aspect ratio [15] $A = (1 + \sqrt{2})$ [19] coincides with B only for $s = 1$, nor does it pertain to the case where $A = 1$.

This work was partially supported by the National Science Council of Republic of China (Taiwan) under the Grant No. NSC 93-2212-M-033-005.

-
- [1] L. Onsager Phys. Rev. 65, 117 (1944).
 [2] W. T. Lu and F. Y. Wu: Physica A 258, 157 (1998); Phys. Lett. A 259, 108 (1999); Phys. Rev. E 63, 026107 (2001).
 [3] B. Kaufman Phys. Rev. 76, 1232 (1949).
 [4] T. D. Schultz, D. C. Mattis and E. H. Lieb, Rev. Mod. Phys. 36, 856 (1964).
 [5] M. Kac and J. C. Ward, Phys. Rev. 88, 1332 (1952).
 [6] H. S. Green and C. A. Hurst, Order-Disorder Phenomena, (Interscience, New York, 1964).
 [7] B. M. McCoy and T. T. Wu, The Two-dimensional Ising Model, (Harvard University Press, Cambridge, MA, 1973).
 [8] V. N. Pleshko: Theor. Math. Phys. 64, 748 (1985); Physica, A 152, 51 (1988); Phys. Lett. A 157, 335 (1991).
 [9] T. M. Liaw, M. C. Huang, S. C. Lin and M. C. Wu, Phys. Rev. B 60, 12994 (1999).
 [10] M. C. Wu and C. K. Hu, J. Phys. A: Math. Gen. 35, 5189 (2002).
 [11] A. E. Ferdinand and M. Fisher, Phys. Rev. 185, 832 (1969).
 [12] M. E. Fisher, in Critical Phenomena, Proceeding of the International School of Physics "Enrico Fermi" Course LI, Varenna on Lake Como, 1970, edited by M. S. Green, (Academic, New York, 1971), Vol. 51, P.1; V. Privman and M. E. Fisher, Phys. Rev. B 30, 322 (1984); Finite-size Scaling, edited by J. L. Cardy, (North-Holland, New York, 1988).
 [13] K. Kaneda and Y. Okabe, Phys. Rev. Lett. 86 2134 (2001).
 [14] R. M. Zi, C. D. Christian and P. Kleban, Physica A 266, 17 (1999).
 [15] Y. Okabe, K. Kaneda, M. Kikuchi and C. K. Hu, Phys. Rev. E 59, 1585 (1999).
 [16] J. Cardy, Nucl. Phys. B 270 [FS16], 186 (1986); J. -B. Zuber, Phys. Lett. 176B, 127 (1986).
 [17] R. Saito, G. Dresselhaus and M. S. Dresselhaus, Physical properties of Carbon Nanotubes, (Imperial College Press, London, 1998).
 [18] N. W. Ashcroft, N. Mermin, Solid State Physics, (Saunders College Publishing, Orlando, Florida, 1976).
 [19] The convention of [15] corresponds to Tw_{II} here.

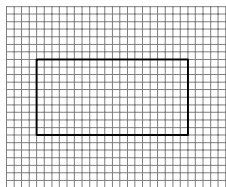
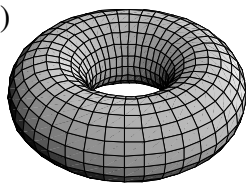
FIG. 1. The formation of helical tori by pairwise joining the edges of the rectangle spanned by any orthogonal set of vectors on the lattice plane: (a) the direction of the primitive vectors coincides with the lattice orientations for the conventional toroidal BC and (b) the helical tori are formed for the non-coincidence.

FIG. 2. Equivalence between the BCs in helical and twisted schemes prescribed by $fa_1; a_2g$ and $fa_1^0; a_2^0g$ respectively, on a $M \times N$ square lattice. For the helical BC, the setting $Q_1=P_1 = Q_2=P_2$ ensures that the two primitive vectors are orthogonal. On the other hand, twisting is generated by a d -unit traverse shift.

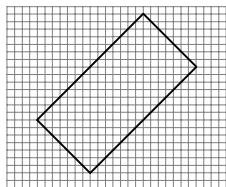
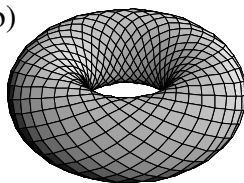
FIG. 3. Plotting $\langle A; \rangle$ against $l=L$ for $A = 1; 2; 3; 4$ with $\theta = 0(^\circ); 0.1A(4^\circ); 0.2A(5^\circ); 0.3A(^\circ); 0.4A(^\circ)$ and $0.5A(^\circ)$. The scaling behaviours are obviously deviated by θ . Nonetheless, for $A = 1$ no splitting is found with respect to the twisting factors.

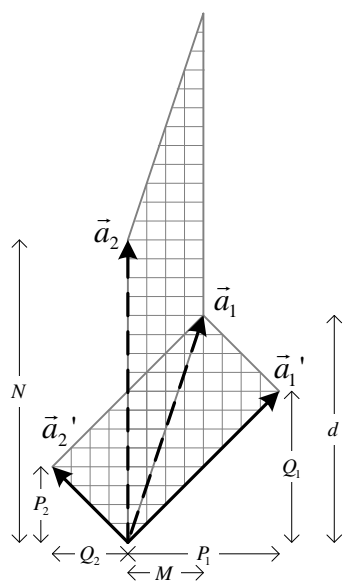
FIG. 4. The plot of $\langle B; \rangle$ versus $l=L$. For a given chiral aspect ratio B . Results of different chiralities collapse into one curve and the curves of both $\langle B; \rangle$ and $\langle l=B; l= \rangle$ versus $l=L$ coincide.

(a)



(b)





This figure "IsingFig3.jpg" is available in "jpg" format from:

<http://arxiv.org/ps/cond-mat/0512262v1>

This figure "IsingFig4.jpg" is available in "jpg" format from:

<http://arxiv.org/ps/cond-mat/0512262v1>